Real-time control of MHD instabilities using ECCD in ASDEX Upgrade

M.Maraschek[1], M.Reich[1], K.Behler[1], L.Giannone[1], A.Gude[1], E.Poli[1],
C.J.Rapson[1], O.Sauter[2], J.Stober[1], W.Treutterer[1], H.Zohm[1],
ASDEX Upgrade team[1] and EUROfusion MST1 team*

[1] *Max-Planck Institut für Plasmaphysik, Boltzmannstr. 2, 85748 Garching, Germany*
[2] *Centre de Recherches en Physique des Plasmas, EPFL, 1015 Lausanne, Switzerland*

Introduction Future tokamaks, like ITER and DEMO, must be capable of controlling neoclassical tearing modes (NTMs) to ensure high β_N plasma operation. These MHD instabilities are performance limiting and in the worst case they are destructive when they trigger a disruption. A proven actuator with which these instabilities can be controlled is electron cyclotron heating and current drive (ECCD) at the rational surface. This requires a precise control of the radial deposition location [1].

In order to achieve this control on ASDEX Upgrade, a large number of real-time (rt) diagnostics and intelligent controllers work in unison, all coordinated by the discharge control system (DCS). The system automatically detects the excitation of magnetic islands and identifies their mode number from magnetic probe signals. It uses electron cyclotron emission (ECE) and magnetic probe signals in combination to infer their radial position. The DCS aims the ECCD at the appropriate rational surfaces in order to stabilize the modes.

A newly introduced method originating at TCV that uses radial sweeps of the ECCD deposition alleviates the precision requirements for ECCD deposition such that inaccurately determined rational surfaces are not prohibitive for NTM stabilization and prevention [2].

Technical upgrades In addition to the essential rt equilibrium reconstruction (typically 4ms, 2ms possible data rate) [3] the controllers require density profile (1ms) [4], detection of MHD marker positions, such as rational surfaces from MHD modes from the electron cyclotron emission (6ms) [5], or the detection of sawteeth [6], ECCD beam-tracing in real-time (15-25ms) [7] and global plasma parameters (such as I_p or β_p from rt-equilibrium) to make their decisions.

Mode detection For the detection of a specific (m/n)-mode with poloidal mode number m and toroidal mode number n a subset of magnetic signals, i.e. $dB_\theta/dt = \dot{B}_\theta$-coils, on the low field (LFS, $\theta = 0^\circ$) and on the high field side (HFS, $\theta = 180^\circ$), are used. From these a set of hardware generated weighted sums, i.e. spatially Fourier filtered signals of the form

$$\dot{B}_{m/n} = \left(\beta_m^{LFS} \frac{\sum_i \alpha_{n,i}^{LFS} \cdot \dot{B}_i^{LFS}}{\sum_i |\alpha_{n,i}^{LFS}|} + \beta_m^{HFS} \frac{\sum_j \alpha_{n,j}^{HFS} \cdot \dot{B}_j^{HFS}}{\sum_j |\alpha_{n,j}^{HFS}|} \right) \Big/ \left(|\beta_m^{LFS}| + |\beta_m^{HFS}| \right)$$

are created. The $\alpha_{n,i}^{xFS}$ define the toroidal mode number n to which the $\dot{B}_{m/n}$ is sensitive, the β_m^{xFS} the dominating odd or even poloidal mode number m. In this way eight frequency independent signals $[n = 1]$, $[n = 2]$, $[n = \text{odd}]$ (sum of two coils on LFS 180° apart), $[n = \text{even}]$ (difference of two coils on LFS 180° apart), $[n = \text{odd}/m = \text{even}]$, $[n = \text{even}/m = \text{odd}]$, $[n = 1/m = \text{even}]$ and $[n = 2/m = \text{odd}]$ are derived in real-time.

These hardware generated $\dot{B}_{m/n}$ signals are used on a rt computer to calculate their amplitude using the envelope and communicating the results to the DCS on a 2ms sample rate. For constant mode frequency, $f_{m/n}(t) = f_{m/n}$, this amplitude is proportional to the island perturbation field.

*See http://www.euro-fusionscipub.org/mst1

The DCS can detect the existence of a (3/2) or a (2/1)-mode by any of these signals and initiate the stabilization attempt at the corresponding rational surface, $\rho_{m/n}$. Locked $n = 1$ modes are identified independently by a set of saddle coils [8]. After the mode has been removed, the gyrotrons can be turned off and are available for other modes. In the future the DCS will decide automatically, which gyrotrons can be most efficiently steered to the resonant surface [9].

Additionally, these mode signals are also connected to the ECE data acquisition system, where they are sampled together with the ECE signals. A correlation analysis is performed to determine the radial location of the phase jump of $\approx \pi$ occurring at the position of the X-point of the island [5]. Together with the rt-equilibrium this provides the radial location, $\rho_{m/n-NTM}(t)$, of the island. For each of the magnetic signals an independent fast Fourier transformation is performed and the frequency, $f_{m/n}(t)$, and amplitude, $A(f_{m/n}(t))$, is determined for $f > 2$kHz. Hence the time evolution of $B_{m/n}(t) \sim A(f_{m/n}(t))/f_{m/n}(t)$ becomes available.

ECCD deposition control The real-time implementation [10, 7] of the beam-tracing code TORBEAM calculates the radial deposition, $\rho_{dep}(t)$, of the ECCD for each of the four gyrotrons individually. The code requires the rt-equilibrium and the rt density profile.

Based on ρ_{dep}, the DCS steers the launching mirrors towards $\rho_{m/n}^{target}$. As the most efficient radial localization, $\rho_{dep}(t)$, of the ECCD with respect to the real resonant surface, $\rho_{m/n}(t)$, and the required accuracy are still open issues, the system provides the possibility to pre-program for each (m/n)-mode a time dependent offset to the radial target,

$$\rho_{m/n}^{target}(t) = \rho_{m/n}(t) + \Delta\rho_{m/n}(t).$$

It is possible to select the radial target trajectory, $\rho_{m/n}(t)$, calculated in real-time, for each gyrotron independently before the discharge. From the rt-equilibrium the radius of the resonant surface, $\rho_{m/n-eq}(t)$, the detection radius from the rt ECE analysis, $\rho_{m/n-NTM}(t)$ and a generic, mode number independent detection radius $\rho_{NTM}(t)$ from the correlation analysis can be selected.

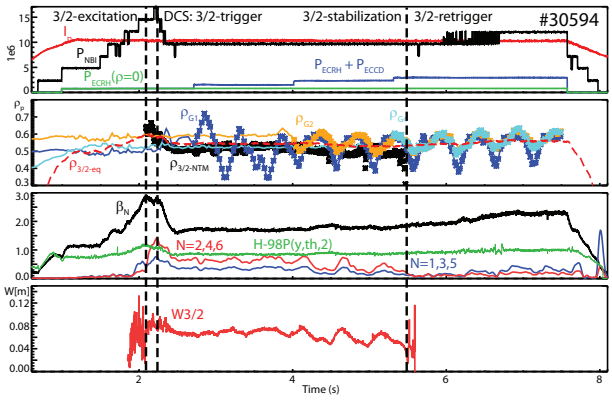

Figure 1: *NTM stabilization using sweeping with 3 P_{ECCD}[MW] steps and attempt to re-trigger mode. first box: I_p[MA] (red), P_{NBI}[MW] (black), central P_{ECRH}[MW] (green) and total $P_{ECRH} + P_{ECCD}$[MW] (blue). second box: $\rho_{3/2-NTM}(t)$ (black symbols), $\rho_{3/2}^{target}(t)$ (blue/orange/cyan lines), $\rho_{ECCD}(t)$ (blue/orange/cyan symbols) from rt-TORBEAM, $\rho_{3/2-eq}(t)$ from rt-equilibrium. third box: $\dot{B}_{n=odd}$ (blue), $\dot{B}_{n=even}$ (red) β_N (black) and H-98P(y,th,2)-factor (green). forth box: island width $W_{3/2}[m]$ (red)*

Island width The island width, $W_{m/n-ECE,ref}$ in m, is calculated from the Fourier filtered ECE amplitude and phase profile at the mode's frequency, $f_{m/n,ref}$[Hz], according to [11]. The profile is considered versus the minor plasma radius, r[m], on the low field side via the equilibrium. With this information from a reference discharge at a reference time (index ref) and the corresponding magnetic measurements, i.e. $\dot{B}_{m/n,ref}$ [T/s], the island width becomes available for discharges with self-similar q-profiles. With the tracked frequency, $f_{m/n}(t)$ [Hz], of a (m/n)-NTM on a single Mirnov coil and its amplitude, $\dot{B}(f_{m/n}(t))$ [T/s], from any discharges the island width

$$W_{m/n}(t) = \left(W_{m/n-ECE,ref} \Big/ \sqrt{\dot{B}_{m/n,ref}/f_{m/n,ref}}\right) \cdot \sqrt{\dot{B}(f_{m/n}(t))/f_{m/n}(t)}$$

is calculated offline for further analysis. This approach is possible, as in all present experiments a plasma current of $I_p = 1.0$MA and a toroidal field of $B_t = -2.5$T have been used.

Experimental setup and scenarios The stabilization experiments have been performed in the improved H-mode or hybrid scenario with $I_p = 1$MA and $B_t = -2.6$T with up to 17.5MW of NBI heating power. One gyrotron is aimed centrally ($\rho_{dep} = 0$), in order to avoid unwanted impurity peaking. This leaves three gyrotrons available for NTM control experiments.

Stabilization scheme For the stabilization scheme, the NBI power is initially ramped up to maximal 17.5MW in order to trigger an NTM. Typically, a (3/2), and occasionally also a (2/1)-NTM is triggered. The natural onset is characterized by $\beta_N^{onset,int}$ and $P_{NBI}^{onset,int}$. Any excited mode triggers the DCS, which switches to different program branch or activates a controller. It reduces the NBI power to typically P_{NBI}^{stab} = 10MW for both the (3/2) and the (2/1)-NTM. Only with $P_{NBI} \leq 10$MW the presently available ECCD power (3 gyrotrons with up to ≈ 2.1MW) for mode stabilization is seen to be able to remove the NTM.

For preemptive NTM avoidance in the same discharge scenario the NBI power is ramped up to an initial P_{NBI} and subsequently the ECCD is applied at the resonant surface, where the first mode is expected, i.e. at the $q = 3/2$-surface. With the preemptive P_{ECCD}^{pre} applied, the NBI power is increased until an NTM is triggered at $P_{NBI}^{onset,pre}$ and $\beta_N^{onset,pre}$.

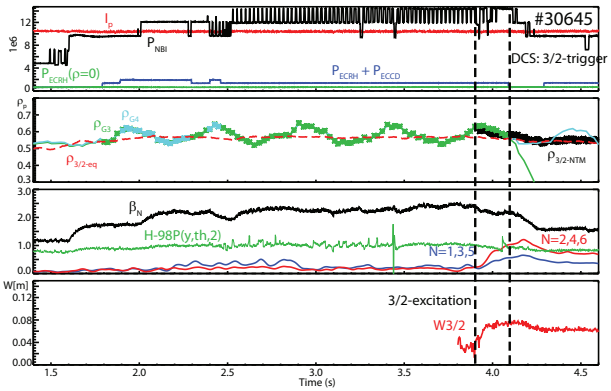

Figure 2: *Preemptive NTM-avoidance using sweeping with one gyrotron ($P_{ECCD}^{pre} \approx 0.65$MW). Traces and colour coding similar as in figure 1.*

Deposition scheme In previous experiments the main aim was to retrieve the optimal value for $\Delta\rho_{m/n}(t) = \Delta\rho_{m/n}$ for the stabilization of NTMs ([12] and references therein). Typically, a slow sweep has been performed to get an estimate for $\Delta\rho_{m/n}$ for subsequent discharges. This approach suffers from the need of a very accurate and reliable determination of $\rho_{m/n}(t)$. The new approach originating at TCV is the use of a triangular sweeping of $\Delta\rho_{m/n}(t)$ centred around the resonant surface estimated from the rt-equilibrium, $\rho_{m/n-eq}(t)$, during the stabilization process. In this case there is always an instant during the sweep when the gyrotron is located optimally for stabilization. This can be identified by the largest island size reduction rate, $\tau_{decay} \sim dW/dt(t) < 0$, during the sweep for small P_{ECCD}. For $P_{ECCD} \geq P_{ECCD}^{stab}$ the mode disappears during the sweep. For an efficient stabilization the sweeprate τ_{sweep} has to be sufficiently large compared to the typical decay time τ_{decay} for optimal radial localization.

For preemptive avoidance of NTMs, sweeping the deposition might be the only possibility. Without the determination of the radial localization, $\rho_{m/n-NTM}(t)$, of an existing (m/n)-mode, only the equilibrium prediction, $\rho_{m/n-eq}(t)$, is available. However, $\rho_{m/n-eq}(t)$ suffers at present from the absence of internal constraints providing information on the q-profile.

Possible caveats of the sweeping technique are a longer required duration of the stabilization compared to an immediately optimal deposition. Also a larger amount of ECCD power, P_{ECCD}^{stab}, might be required, as the time integrated driven current within the island is lower.

Stabilization of a (3/2)-NTM with sweeping of $\rho_{m/n}^{target}(t)$ In discharge #30594 (figure 1)

three gyrotrons are subsequently activated with a delay of 1.3s in the intermediate $P_{NBI} = 10$MW phase. A (3/2)-NTM is triggered in the high $P_{NBI}^{onset,int} = 17.5$MW phase at $\beta_N^{onset,int} = 2.8$. During the 1.3s period with constant P_{ECCD} the sweeping of ρ_{ECCD} is applied to all three gyrotrons and therefore a three step power scan has been achieved. Only with the maximal $P_{ECCD}^{stab} = 2.1$MW the (3/2)-NTM disappears during the first sweep of ρ_{ECCD} over $\rho_{3/2-NTM}$. After the removal of the (3/2)-NTM a maximal $\beta_N = 1.8$ has been achieved with $P_{NBI} = 10$MW. A subsequent rise of P_{NBI} up to 12.5MW and $\beta_N = 2.3$ did not retrigger an NTM, as the ECCD in its sweeping mode was preemptively avoiding the reexcitation.

Preemption of (3/2)-NTM with sweeping Compared to previous preemptive experiments [3], figure 2 shows discharge #30645, where with only one radially sweeping gyrotron, i.e. $P_{ECCD}^{pre} = 0.65$MW the excitation of an NTM with $P_{NBI} = 12.5$MW could be avoided. Only during a P_{NBI}-ramp at $P_{NBI}^{onset,pre} = 15$MW at $\beta_N^{onset,pre} = 2.45$ a (3/2)-NTM gets excited. The otherwise identical comparison discharge without ECCD showing an earlier NTM excitation at lower P_{NBI} and β_N is still missing. However, typically at these β_N values NTMs are excited.

Summary and outlook Several updates, which have been included in the setup for MHD control at ASDEX Upgrade have been reported. A major new development has been a continuous sweep of the ECCD deposition around the resonant surface, $\rho_{m/m-eq}$, both for NTM stabilization and preemptive avoidance. This technique relaxes the requirements on the accuracy of the localization of the ECCD. It has enabled us to perform NTM avoidance in new scenarios, without predetermination of the exact $q = m/n$ position based on preparation discharges. In the future, a definition of a generic figure of merit is required, to make the efficiency of stabilization and avoidance and also modes with different mode numbers directly comparable.

Stabilization of multiple modes, amplitude based stabilization, sawtooth tailoring and disruption avoidance are further examples of the generic capabilities of specialized controllers of the ASDEX Upgrade DCS, which will be further optimized for its joint application in ITER.

References

[1] C. C. Hegna and J. D. Callen, Phys. Plasmas **4**, 2940 (1997).
[2] D. Kim et al., in *55th An. APS Meeting of the Div. of Plasma Physics*, page PP8.00073, 2013.
[3] L. Giannone et al., Fusion Engineering and Design **88**, 3299 (2013).
[4] A. Mlynek et al., Nuclear Fusion **51**, 043002 (2011).
[5] M. Reich et al., Fusion Eng. Design **61**, 309 (2012).
[6] A. Gude et al., in *Proc. of the 42nd EPS Conf. on Plasma Physics*, page P1.122, 2015.
[7] M. Reich et al., in *Proc. of the 25th IAEA Conference Fusion Energy, 2014*, pages IAEA–CN–221/PPC/P1–267, 2014.
[8] M. Maraschek et al., in *Proc. of 40th EPS Conf. on Plasma Phys.*, page P4.127, 2013.
[9] C. J. Rapson et al., Fusion Eng. Design , online: http://dx.doi.org/10.1016/j.fusengdes.2015.01.007 (2015).
[10] M. Reich et al., Fusion Eng. Design , online: http://dx.doi.org/10.1016/j.fusengdes.2015.04.024 (2015).
[11] J. P. Meskat et al., Plasma Physics and Controlled Fusion **43**, 1325 (2001).
[12] M. Reich et al., in *Proc. of the 40th EPS Conf. on Plasma Physics*, page P2.151, 2013.

Acknowledgement *This work has been carried out within the framework of the EUROfusion Consortium and has received funding from the Euratom research and training program 2014-2018 under grant agreement No 633053. The views and opinions expressed herein do not necessarily reflect those of the European Commission.*